Study on the adhesive property of sludge-modified magnesium phosphate cement reinforcement coating for steel bars

Zhang Shusen[1], Yang Jiapeng[2]*, Li Yiyang[2], Wang Zhenyu[1], Zhong Shunjie[3], Zhuang Liling[3] and Wang Tao[1]

[1]Cangzhou Qugang Expressway Construction Co., Ltd., Cangzhou, Hebei, China, [2]School of Civil Engineering, Tianjin University, Tianjin, China, [3]Fujian Zhanglong Construction Investment Group Co., Ltd., Zhangzhou, Fujian, China

The synergistic interaction inreinforced concrete systems originates from the strong bond between steel reinforcement and concrete, enabling them to collaborateunder load and optimize structural performance. This study applied various sludge-modified magnesium phosphate cement mixtures to the surfaces of plain round steel bars and ribbed steel bars to prepare steel-reinforced concrete specimens. The characterization of the bond performance of the sludge-modified magnesium phosphate cement reinforcement coating for steel bars and concrete was achieved through analyzing the failure modes, bond strength, and slip values of different groups. Microscopic analysis was performed using a scanning electron microscope. The results revealed that the primary failure mode of the steel-reinforced concrete specimens was steel bar pull-out, with some specimens exhibiting concrete splitting failure. Coating application on plain round steel bars increased bond strength, while on ribbed steel bars, it decreased bond strength. The application of the coating slightly reduced slip values to some extent.

1 Introduction

The reinforced concrete system can form a good working system cooperation work because there is a good bond between the steel bar and the concrete. The steel bar and concrete can work together when the force is loaded, and the best structural performance of the system can be observed. Good adhesive properties guarantee the most basic safety, shock resistance, durability, maintenance, and operating costs of reinforced concrete structures and quality control during construction. There is a good bond stress between the reinforcement and concrete, which is generally provided by the following aspects (Zhao and Jin, 2002; Yang et al., 2013; Haque and Chen, 2019; Nobre et al., 2020).

In reinforced concrete structures, bonding stress between the concrete and steel reinforcement is primarily facilitated by chemical adhesion, mechanical

bite force, and friction. Chemical adhesion results from the hydration reaction of cement with steel surfaces, forming a solid interface. Mechanical bite force, especially crucial for ribbed steel bars, relies on surface properties and internal pressure to enhance the bond strength. Friction force, generated when concrete envelops steel bars and resists relative movement, is influenced by extrusion pressure, surface roughness, and concrete shrinkage. Chemical bonding is typically minimal, with round bars relying more on friction and ribbed bars on mechanical bite force for effective bonding (Jiang and Qiu, 2012; Yang, 2018; Szewczak et al., 2020).

Magnesium phosphate cement (MPC) differs from traditional Portland cement, possessing unique hydration and hardening characteristics (Bodong et al., 2023; Xiangrui et al., 2023; Xin et al., 2022). Due to its ceramic-like properties, MPC is also referred to as chemically bonded magnesium phosphate ceramics. MPC is typically produced through an acid–base neutralization reaction between calcined magnesium oxide and water-soluble acid phosphate. It offers several advantages, including rapid setting and hardening, high early strength, good volumetric stability, strong bond strength, and excellent resistance to chloride and sulfate ions. These properties make MPC widely applicable in structural repair and reinforcement, bioceramics, radioactive and hazardous waste containment, manufacturing embedded mold materials, and protective coatings. MPC is particularly favored for use in protective coatings due to its unique combination of fast hardening, strong adhesion, and superior fire and corrosion resistance. Recent studies have further demonstrated that MPC exhibits a high degree of similarity with ordinary Portland cement in terms of the thermal expansion coefficient and volume compatibility. As a result, MPC is well-suited for producing anti-corrosion coatings to protect reinforced concrete from degradation (Wang et al., 2021; Jun et al., 2019; Kytinou et al., 2020; Xiaoming et al., 2023; Zhang et al., 2023).

Yang Haiyan applied a magnesium phosphate cement coating with a thickness of approximately 500 μm on the surface of Q235 steel (Yang, 2018). Through electrochemical tests and salt spray tests, it was proven that the magnesium phosphate cement coating has a good anti-corrosion protection effect on Q235 steel, and the magnesium phosphate cement coating with the combination of silica ash and Al_2O_3 is better in corrosion resistance. Li studied the sulfate attack resistance of concrete coated with coating, magnesium phosphate cement coating, and epoxy coating, and the results indicated that the structure and composition of the MPC coating changed under the sulfate attack environment. The MPC coating made concrete bonds more tightly, and the structure was more compact than in other environments, which significantly corroded the sulfate protection effect of concrete. The MPC coating can significantly improve the sulfate resistance of concrete than epoxy coating (Jun et al., 2019). Tang studied the protective effect of magnesium phosphate cement on steel corrosion in the restoration of reinforced concrete structures, and the results indicated that MPC has a good protective effect on steel corrosion, which might be due to the newly formed protective film on the steel surface. In addition, the related reactions between phosphate and $Fe^{2}+$ ions may play an important role in the formation of the protective film and effectively reduce the corrosion rate (Tang et al., 2020). Yang Quan Bing studied the ability of magnesium phosphate cement mortar, ordinary

Portland cement, and slag cement to prevent corrosion of steel bars. The results indicated that after six dry–wet cycles, the corrosion rate of magnesium phosphate cement mortar was only 0.18%, which was only 22.8% of that of ordinary Portland cement and 48.6% of that of slag cement (Yang et al., 2000). Xiangdong made a reinforced concrete specimen coated with epoxy coating. By controlling the steel bar diameter and effective bond length, the influence on the bond performance of the specimen was analyzed, and the relevant bond strength calculation formula was proposed (Yang, 2018). Jones analyzed and studied the influence of various factors on the bond strength between epoxy-coated steel bars and high-performance concrete. Based on the analysis of these data, he put forward relevant suggestions for modifying the current formula (Jones and Ramirez, 2016). Zhang conducted a pull-out test on the bond performance of FRP bars and concrete and analyzed the bond slip constitutive model of ribbed FRP bars and plain bars. The failure forms of the specimens are sliding and pulling out of FRP bars and breaking of FRP bars. With the decrease in the surface reinforcement and anchorage length of FRP bars and the increase in concrete strength, the average bond strength between FRP bars and concrete increases (Yongkang and Xiaoming, 2012).

Sludge, as an inert admixture, can be used to modify magnesium phosphate cement, effectively extending its setting time and enhancing its early mechanical properties. Additionally, sludge can be applied directly as an anti-corrosion coating on the surface of steel bars, providing significant protection and improving their corrosion resistance. However, there is limited research on the adhesive properties between sludge-modified magnesium phosphate cement coatings and concrete. Therefore, this study employs pull-out tests as the core experimental framework to evaluate and analyze the adhesive properties of modified magnesium phosphate cement coatings with varying sludge contents by preparing pull-out test specimens (Ryu et al., 2024; Guan et al., 2024; Furong et al., 2024; Pavlíková et al., 2020).

2 Materials and methods

2.1 Experimental material

The re-fired magnesia produced by Jinan Ludong Refractory Material Co., Ltd. is calcined and ground into magnesia powder at 1700°C for the preparation of magnesia phosphate cement. The powder is brownish yellow. Potassium dihydrogen phosphate (KH_2PO_4) produced by Sinophosphate Chemical Reagent Co., LTD. is a white powder, easily soluble in water at room temperature. Prior to experimentation, the sludge obtained from the desiccation project at Yuecheng Reservoir in Cixian County, Handan City, Hebei Province, requires activation. The activation process involves drying the sludge in a drying box, followed by ball milling to produce a brown and yellow powder. Subsequently, the powder undergoes calcination in a high-temperature furnace before being subjected to ball milling again. The chemical composition of the resulting material is detailed in the table below. The chemical composition of the material is shown in Tables 1, 2 (Lv et al., 2024a; Lv et al., 2024b; Lv et al., 2024c).

P.O.42.5 ordinary Portland cement, produced by the Tangshan Yanshan Cement Factory, was selected for the concrete preparation.

TABLE 1 Chemical composition of MgO (%).

MgO	SiO$_2$	CaO	Fe$_2$O$_3$	Al$_2$O$_3$	Loi
89.65	5.18	2.94	1.04	1.04	1.03

Crushed stone and river sand were used as aggregates, with the stone having a uniform particle size range of 5–25 mm and the river sand featuring continuous grading with a maximum particle size of 5 mm. The chemical composition of the cement is presented in Table 3 below.

2.2 Mix ratio design

Due to the small particle size of the sludge, even a small amount can significantly affect the flow behavior of the MPC system. Therefore, in this study, while varying the sludge content in different groups, the flowability of each group was kept consistent. The MG-P molar ratio of the magnesium phosphate cement in the sludge-free group was maintained at 8.5, and the combined mass of the sludge and MgO in the sludge-containing groups was controlled to 2.5, ensuring uniform fluidity across all groups. The specific proportions of MPC with varying sludge contents used in the experiment are presented in Table 4. Additionally, uncoated steel bars (Group C) were prepared as a control group.

The concrete design strength of the drawing specimen is C40 concrete, and the mix ratio per cubic meter of concrete is calculated according to JG55-2011"Ordinary Concrete Mix ratio Design Regulations", as shown in Table 5 below.

2.3 Specimen preparation

Production of magnesium phosphate cement: Magnesium phosphate cement is prepared according to the modified mix ratio detailed in Table 4. Initially, the required amounts of magnesium oxide, phosphate, and sludge are weighed according to the ratios specified. These materials are then placed into a cement slurry mixer and mixed at a slow speed for 60 s to ensure thorough and uniform blending of the dry components. Next, water, measured according to the mix ratio, is added to the mixer and stirred at a slow speed for another 60 s. The mixing is paused, and any remaining material adhering to the blade and walls of the pot is scraped down into the mixer by using a shovel. The mixture is then stirred for an additional 60 s to achieve uniform consistency. After mixing, the modified magnesium phosphate cement is ready for use.

Coating steel bar production: Given the rapid setting and hardening characteristics of magnesium phosphate cement, the coating process must be executed promptly. First, the prepared magnesium phosphate cement is introduced into a semi-circular PVC pipe. The steel bar is then rotated within the PVC pipe to ensure a complete and even coating of the magnesium phosphate cement on its surface. Finally, the mixing pot and PVC pipe are thoroughly cleaned to remove any residual material.

Coating of steel bars: Due to the rapid setting and hardening of MPC, the coating process should be performed swiftly, with

the entire operation completed within 5 min. First, the prepared MPC is placed into a semi-circular PVC pipe, and the steel bar is rotated within the PVC pipe to ensure that the surface is uniformly coated with MPC. The consistent flowability of the slurry ensures a uniform coating thickness of approximately 1 mm. The coated steel bars are then cured under indoor air conditions (25°C ± 2°C, RH 70% ± 5%). Finally, the mixing bowl and PVC pipe are thoroughly cleaned.

Drawing test piece production: For the preparation of drawing test pieces for reinforced concrete, use steel bars with a diameter of 10 mm and a length of 500 mm, and pour concrete into molds to create cubes measuring 150 mm × 150 mm × 150 mm. Insert one end of the steel bar into the mold to a depth of 100 mm, with the other end extending 250 mm, and set the protective layer thickness to 75 mm. To minimize experimental errors, place a PVC pipe of 50 mm length at each end of the steel bar. The effective bonding length between the steel bar and concrete is set to 5 d (where d is the diameter of the steel bar; thus, 5 d equals 50 mm). The specific mold is depicted in Figure 1. First, apply a release agent to the inside of the plastic mold. Next, accurately weigh the required amounts of cement, aggregate, and sand according to the mix ratio, and combine them in the concrete mixing pot. Perform a dry mix for 90 s to ensure uniform distribution of the dry materials. Add the measured water, and mix until the concrete achieves the desired flow and consistency. Pour the mixed concrete into the pre-oiled plastic mold, position the mold in the center of a shaking table, and use a scraper to remove excess concrete while vibrating the mold to ensure proper compaction.

2.4 Experimental method

The central drawing test device used a WAW-1000A microcomputer controlled electro-hydraulic servo universal testing machine to load the specimen and customized the drawing fixture with matching size according to the specifications of the loading device. Before loading, the specimen was passed through the drawing fixture, the upper end of the loading test machine tightened the fixture, and the lower end of the clamping steel bar loading device is shown in Figure 2 below. The loading mode was set as displacement loading, and a dial gage was fixed at the free end of the reinforced concrete specimen to test the relative slip between the reinforcement and concrete. During the experiment, when the free slip end exceeds the specified value, the concrete cracks or the steel bar is pulled apart, the loading is stopped and the load and the dial indicator are recorded at this time, and then the loading of the next specimen is continued.

Scanning electron microscopy (SEM) was used to analyze the magnesium phosphate cement modified with different amounts of sludge and to explain the influence on the adhesive properties at the microscopic level. The EDS point spraying method was used to analyze the chemical element composition of the modified magnesium phosphate cement and to explain the effect of the modified magnesium phosphate cement with different amounts of sludge.

TABLE 2 Chemical composition of sludge (%).

Al_2O_3	SiO_2	Fe_2O_3	CaO	MgO	CO_2	Na_2O	Loi
17.3	56.1	7.9	9.2	3.3	5.9	0.3	5.9

TABLE 3 Chemical composition of cement (%).

Al_2O_3	SiO_2	Fe_2O_3	CaO	MgO	SO_3	f-CaO	Loi
5.03	20.58	3.38	63.32	2.01	2.06	0.68	1.76

TABLE 4 Design of the mixing ratio of sludge-modified magnesium phosphate cement.

Number	MgO (%)	Sludge (%)	Water cement ratio	MgO + sludge/KH_2PO_4
MS-0	100	0	0.23	
MS-5	95	5	0.235	
MS-10	90	10	0.24	
MS-15	85	15	0.25	2.5
MS-20	80	20	0.26	
MS-25	75	25	0.27	
MS-30	70	30	0.275	

TABLE 5 Concrete mix design (kg/m^3).

Cement	Pebble	Sand	Water
500	750	900	200

FIGURE 1
Specimen mold.

FIGURE 2
Experimental loading.

FIGURE 3
Center pull-out failure.

FIGURE 4
Bond strength of the round steel bar.

3 Results and discussion

3.1 Failure mode

During the experimental loading, all 24 pull-out specimens of circular steel bars exhibited central pull-out failure, as illustrated in Figure 3. This indicates that there was a slip between the steel bars and the concrete, and the PVC pipes at both ends of the steel bars also experienced some degree of slip. This failure mode suggests that the friction force between the steel bars and the concrete was insufficient to overcome the applied tensile stress, leading to the direct pull-out of the steel bars due to low bond strength. For the 24 ribbed steel bar pull-out specimens, those with a coating on the surface also displayed central pull-out failure. However, the specimens with uncoated surfaces exhibited splitting failure, primarily due to the high mechanical bite force between the ribs of the ribbed steel bars and the concrete. This high bond strength between the steel bars and concrete is maintained until the tensile stress of the concrete exceeds its tensile and cracking strength, resulting in splitting failure. When the surface of the ribbed steel bars is coated, the mechanical bite force between the ribs and the steel bars is disrupted. In all groups, there was no evidence of peeling or detachment between the magnesium phosphate cement coating and the steel bars, indicating that the bond strength between the magnesium phosphate cement and the steel bars is robust. This suggests that the coating adheres well to the steel bar surface, providing effective protection (Yang et al., 2002; Li et al., 2021).

3.2 Bond strength

Since the central drawing test was used for test loading in all experiments and the length of the bonding section between reinforcement and concrete was small, the bonding stress between
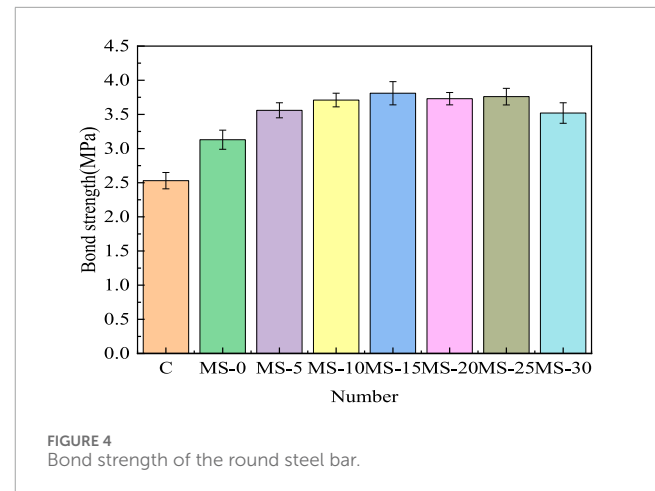
the reinforcement and concrete was approximately regarded as uniformly distributed, and the following Formula 1–1 was used to calculate the bonding stress. The labels MS-0, MS-5, MS-10, MS-15, MS-20, MS-25, and MS-30 represent the sludge contents of 0, 5%, 10%, 15%, 20%, 25%, and 30%, respectively.

$$\tau = \frac{P}{\pi dl}. \tag{1}$$

In the above formula, τ represents the calculated bond stress, and the unit is MPa.
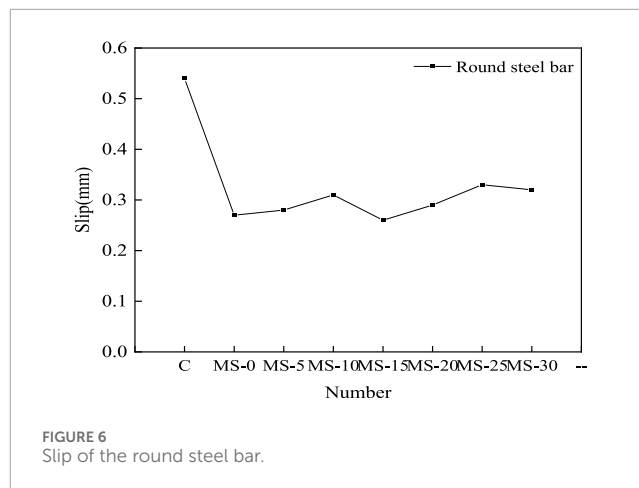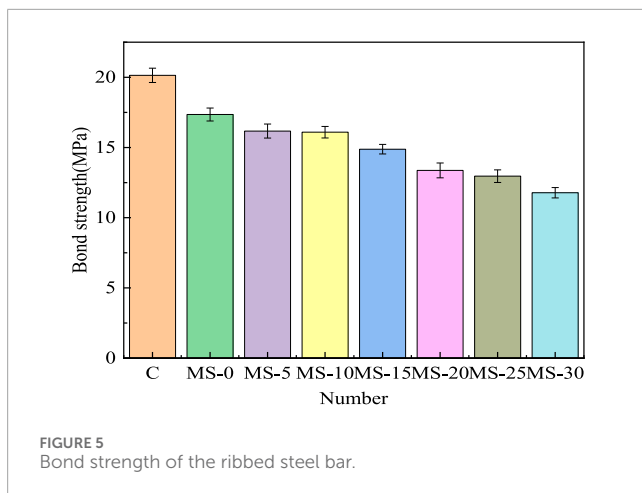
P represents the measured drawing force, and the unit is N.

d represents the diameter of the coated steel bar, expressed in mm.

l is the length of the effective bonding section, expressed in mm.

The bond strength of modified magnesium phosphate cement with varying sludge contents, applied to smooth round steel bars, is illustrated in Figure 4. Without the magnesium phosphate cement coating, the bond strength of the smooth round steel bar is the lowest, at 2.53 MPa. With the addition of sludge at 0%, 5%, 10%, 15%, 20%, 25%, and 30%, the bond strengths increased to 3.13 MPa, 3.56 MPa, 3.71 MPa, 3.81 MPa, 3.73 MPa, 3.76 MPa, and 3.52 MPa, respectively. The corresponding bond strength increases were 23.7%, 40.7%, 46.6%, 50.6%, 47.4%, 48.6%, and 39.1%, respectively. These data indicate that the inclusion of sludge significantly enhances the bond strength between the modified magnesium phosphate cement-coated steel bars and concrete, with the optimal bond performance achieved at a sludge content of 15%. However, further increases in sludge content have a diminishing effect on bond performance. The observed improvement in bond strength with the magnesium phosphate cement coating is primarily due to the increased friction force between the smooth steel bars and the concrete, which is related to the roughness of the contact surface. The coating introduces surface irregularities and pores, which enhance bond strength. Additionally, research by Tang Hao supports these findings, highlighting that magnesium phosphate cement exhibits strong adhesive properties with steel bars and forms a dense bonding layer on the steel surface, further contributing to the increased bond strength observed with the coating (Tang et al., 2020).

The bond strength of modified magnesium phosphate cement applied to ribbed steel bars with varying sludge contents is depicted in Figure 5. The data clearly show that the bond strength behavior

FIGURE 5
Bond strength of the ribbed steel bar.

FIGURE 6
Slip of the round steel bar.


FIGURE 7
Slip of the ribbed steel bar.

of ribbed steel bars is opposite to that of smooth round steel bars. For ribbed steel bars without coating, the bond strength is the highest at 21.83 MPa. As sludge is added, the bond strength of the ribbed steel bars gradually decreases. Specifically, with sludge contents of 0%, 5%, 10%, 15%, 20%, 25%, and 30%, the bond strengths are 17.35 MPa, 16.17 MPa, 16.09 MPa, 14.88 MPa, 13.37 MPa, 12.96 MPa, and 11.78 MPa, respectively. The reductions in bond strength are 20.5%, 25.9%, 26.3%, 31.8%, 38.8%, 40.6%, and 46.0%, respectively. The significant reduction in the bond strength of coated ribbed steel bars is attributed to the disruption of the mechanical biting force between the ribs and the concrete. In uncoated ribbed steel bars, the bond strength is primarily supported by this mechanical biting force. However, when the modified magnesium phosphate cement coating is applied, it interferes with the biting force, leading to a reliance on friction force and the diminished mechanical bite force, ultimately reducing the overall bond strength (Mathern and Yang, 2021; Chen et al., 2023).

Comparing the two types of steel bars reveals that the adhesive properties of smooth round steel bars improve with the application of modified magnesium phosphate cement coating. Conversely, the adhesive properties of ribbed steel bars decrease with the same coating. This difference is primarily related to the nature of the bond between each type of steel bar and the concrete. While coating ribbed steel bars in engineering applications can enhance their corrosion protection, it may also lead to a reduction in bond strength. Therefore, a careful evaluation and analysis are necessary to balance the benefits of improved corrosion resistance with the potential decrease in bond strength during application.

3.3 Slippage

Figure 6 illustrates the slippage of smooth round steel bars coated with modified magnesium phosphate cement containing varying sludge contents. For smooth round steel bars, the bond stress between the steel bar and the concrete is primarily provided by friction force. The data show that the slip amount for uncoated steel bars is the largest, reaching 0.54 mm. When modified magnesium phosphate cement is applied, the slip amount decreases significantly.
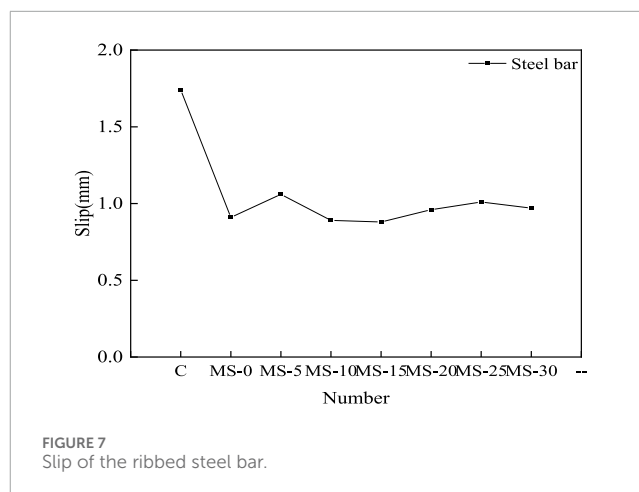
Specifically, for sludge contents of 0%, 5%, 10%, 15%, 20%, 25%, and 30%, the slip amounts are 0.27 mm, 0.28 mm, 0.31 mm, 0.26 mm, 0.29 mm, 0.33 mm, and 0.32 mm, respectively. Analysis of the different sludge contents indicates that there is minimal variation in the slip amount across the different groups, suggesting that the sludge content has little impact on the slip of the modified magnesium phosphate cement-coated round steel bars. During the test loading process, there is no significant slip observed in the initial stages; however, as loading progresses, the uncoated group experiences substantial slip due to inadequate bonding force between the steel bar and the concrete. Coating the steel bar surface improves the roughness of the contact surface, thereby reducing slip when the maximum load is reached. Overall, applying a modified magnesium phosphate cement coating to the surface of smooth round steel bars effectively enhances the bond strength between the steel bar and concrete, reducing relative slip. This treatment not only improves the corrosion resistance of the steel bars but also increases the bond strength with the concrete (Xiang and Yang, 2023; He and Lu, 2024a).

Figure 7 illustrates the slippage of ribbed steel bars coated with modified magnesium phosphate cement containing various sludge contents. For ribbed steel bars, the bond stress is primarily provided by the mechanical biting force between the ribs and the
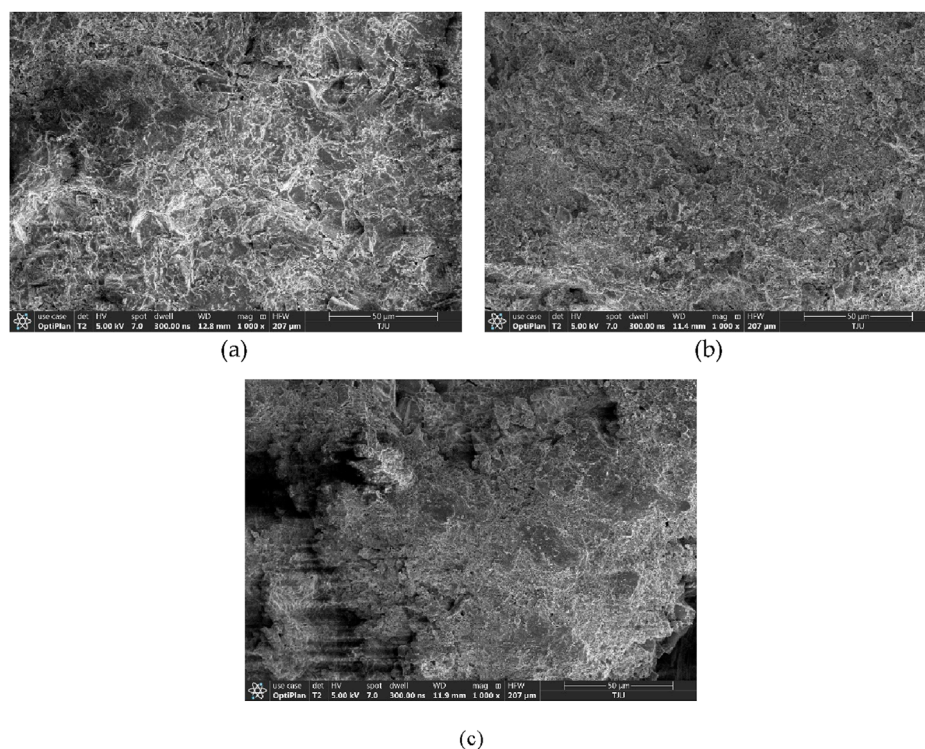
FIGURE 8
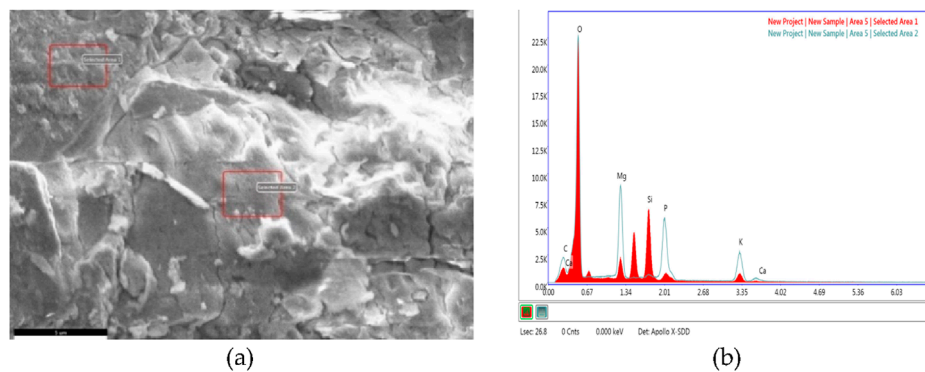SEM images of MPC modified by sludge **(A)** 0%; **(B)** 15%; and **(C)** 30%.

FIGURE 9
EDS test **(A)** test area and **(B)** elemental analysis.

concrete. The slip amount for the uncoated group is 1.74 mm. With the application of modified magnesium phosphate cement coating, the slip amount decreases to some extent. Specifically, with sludge contents of 0%, 5%, 10%, 15%, 20%, 25%, and 30%, the slip amounts are 0.91 mm, 1.06 mm, 0.89 mm, 0.88 mm, 0.96 mm, 1.01 mm, and 0.97 mm, respectively. The sludge content has a minimal effect on the slippage of ribbed steel bars, similar to the trend observed with smooth round steel bars. Ribbed steel bars, due to their threaded surface, generate significant mechanical biting force with the concrete. However, when the surface of the steel bars is coated, the uniform coating reduces the mechanical biting force between the coated steel bars and the concrete, which diminishes

the bond performance and decreases slip amount. Consequently, the slip amount is reduced when the maximum load is reached (He et al., 2024; He and Lu, 2024b).

When smooth round and ribbed steel bars are uncoated, the slip amount of the smooth round steel bar is relatively small. This is due to the lower bond strength between the smooth round steel bar and the concrete, resulting in minimal slip when the loading process reaches its maximum load. After coating, the slippage of both types of steel bars decreases, indicating that the coating effectively reduces the relative slippage between the steel bars and the concrete. This reduction in slip contributes to improved structural stability.

3.4 Microanalysis

Figure 8 displays SEM images of modified magnesium phosphate cement with varying sludge contents. The images reveal that struvite, the primary hydration product of magnesium phosphate cement, predominantly exhibits a sheet-like structure. The overall structure consists of a spatial arrangement formed by magnesium oxide and struvite, which has not undergone further hydration. Comparison of SEM images across different sludge contents shows that pure magnesium phosphate cement has notable voids and large pores. At a sludge content of 15%, the overall compaction of the structure significantly improves. However, as the sludge content increases to 30%, the amount of struvite decreases, and some voids and pores become evident. This phenomenon is primarily due to the fact that the main component of sludge is inactive quartz (SiO_2), and the sludge particles are small. On one hand, the inactive sludge can adhere fully to the surface of magnesium oxide, extending the time the water remains in contact with the material, which enhances the hydration reaction. This leads to the formation of more guanolite, increasing the density and reducing porosity. On the other hand, the small particle size of the sludge allows it to function as an inactive filler material, filling gaps between struvite and magnesium oxide. This increases the overall density of the structure and further reduces porosity. However, when the sludge content is too much, it will replace part of the amount of magnesium oxide, resulting in insufficient reaction material and a reduction in the amount of struvite as a hydration product. Through SEM analysis, it is explained that the bond strength of the smooth round steel bar reaches the maximum when the sludge content is 15%, but decreases when the sludge content is 30%.

Figure 9 presents the correlation analysis of modified magnesium phosphate cement with 30% sludge content, conducted via EDS point scanning. The analysis reveals that as the sludge content increases, the proportion of silicon (Si) in the cement matrix increases. This is attributed to the high SiO_2 content in the sludge, which causes a decrease in the magnesium-to-phosphorus (Mg/P) ratio. After 7 days of curing, the Si content in region 1 of the sample with 30% sludge is 18.46%. This indicates that excessive sludge can displace magnesium oxide, leading to an insufficient amount of magnesium oxide and resulting in inadequate hydration reactions. Consequently, there is a reduced formation of struvite, leading to a less complete structure with numerous pores and cracks. Additionally, the excess sludge negatively impacts structural densification and reduces the bond strength of the smooth round steel bars.

4 Conclusion

(1) The primary failure mode of the reinforced concrete specimens is reinforcement pull-out failure, with some groups exhibiting concrete splitting failure. This occurs mainly because the friction between the circular steel bars (both coated and uncoated) and the concrete is insufficient to overcome the applied tensile stress, leading to pull-out failure. However, ribbed steel bars experience splitting failure due to the high mechanical interlock force between the ribs and the concrete.

(2) Based on the bond strength analysis of each group, the bond strength of smooth round steel bars improves after coating, primarily due to the increased roughness of the contact surface, which enhances friction and bond strength. In contrast,

coating ribbed steel bars reduces their bond strength, as the coating disrupts the mechanical interlock between the ribs and the concrete, weakening the bond.

(3) Analysis of the slip amounts for each group shows that applying a modified coating to the steel bar surface reduces slippage to some extent. However, the sludge content generally has little impact on slip amounts, as the coating alters the friction and mechanical interlock between the steel bar and concrete, which in turn affects slippage.

(4) According to SEM/EDS microscopic analysis, the main components of magnesium phosphate cement are magnesium oxide and struvite. The addition of sludge acts as a filler, reducing porosity and increasing the densification of the cement. However, excessive sludge can introduce cracks and voids. EDS spectrum analysis indicates that as sludge content increases, the proportion of silicon (Si) also increases, which leads to reduced magnesium oxide content and an incomplete hydration reaction, resulting in insufficient struvite formation.

Data availability statement

The original contributions presented in the study are included in the article/Supplementary Material; further inquiries can be directed to the corresponding author.

Author contributions

ZaS: conceptualization, methodology, project administration, visualization, and writing–review and editing. YJ: conceptualization, resources, supervision, and writing–review and editing. LY: funding acquisition and writing–original draft. WZ: validation and writing–original draft. ZoS: validation and writing–original draft. ZL: data curation, validation, and writing–original draft. WT: validation, visualization, and writing–review and editing.

Funding

Conflict of interest

Authors ZaS, WZ, and WT were employed by Cangzhou Quangang Expressway Construction Co., Ltd. Authors ZoS and ZL were employed by Fujian Zhanglong Construction Investment Group Co., Ltd.

The remaining authors declare that the research was conducted in the absence of any commercial or financial relationships that could be construed as a potential conflict of interest.

Publisher's note

References

Bodong, F., Zhuojun, H., Tao, S., Yanming, L., Xian, W., Daping, Y., et al. (2023). Research progress on the properties and applications of magnesium phosphate cement. *Ceram. Int.* 49 (3), 4001–4016. doi:10.1016/j.ceramint.2022.11.078

Chen, Y., Wang, Z., Lin, Y., Wang, H., and Hua, L. (2023). Theoretical modeling and experimental verification of the bending deformation of fiber metal laminates. *Materials* 16 (9), 3486. doi:10.3390/ma16093486

Furong, L., Guoxing, C., Guizhong, X., and Yongyi, W. (2024). An experimental study on the compressive dynamic performance of polypropylene fiber reinforced concrete for retaining structure under automobile collision magnitude. *Adv. Civ. Eng.* 2020. doi:10.1155/2020/8826006

Guan, G., Wang, X., Xin, M., Sun, C., Zhang, Q., and He, J. (2024). Study on the bonding performance of BFRP bars with seawater sand concrete. *Materials* 17 (3), 543. doi:10.3390/ma17030543

Haque, M. A., and Chen, B. (2019). Research progresses on magnesium phosphate cement: a review. *Constr. Build. Mater.* 211, 885–898. doi:10.1016/j.conbuildmat.2019.03.304

He, R., and Lu, N. (2024a). Air void system and freezing-thawing resistance of concrete composite with the incorporation of thermo-expansive polymeric microspheres. *Constr. Build. Mater.* 419, 135535. doi:10.1016/j.conbuildmat.2024.135535

He, R., and Lu, N. (2024b). Hydration, fresh, mechanical, and freeze-thaw properties of cement mortar incorporated with polymeric microspheres. *Adv. Compos. Hybrid Mater.* 7 (3), 92. doi:10.1007/s42114-024-00899-2

He, R., Nantung, T., and Lu, N. (2024). Unraveling microstructural evolution in air-entrained mortar and paste: insights from MIP and micro-CT tomography amid cyclic freezing-thawing damage. *J. Build. Eng.* 94, 109922. doi:10.1016/j.jobe.2024.109922

Jiang, D., and Qiu, H. (2012). Test study on bonding performance of reinforced concrete anchorage zone under repeated loads, 33(9), 127–135.

Jones, J., and Ramirez, J. A. (2016). Bond of reinforcement in high-strength concrete. *ACI Struct. J.* 113 (3), 549–556. doi:10.14359/51688620

Jun, L., Yongsheng, J., Linglei, Z., and Benlin, L. (2019). Resistance to sulfate attack of magnesium phosphate cement-coated concrete. *Constr. Build. Mater.* 195, 156–164. doi:10.1016/j.conbuildmat.2018.11.071

Kytinou, V. K., Chalioris, C. E., and Karayannis, C. G. (2020). Analysis of residual flexural stiffness of steel fiber-reinforced concrete beams with steel reinforcement. *Materials* 13 (12), 2698. doi:10.3390/ma13122698

Li, H., Guo, X., and Duan, J. (2021). Numerical simulation of steel-reinforced reactive powder concrete beam based on bond-slip. *Materials* 14 (15), 4176. doi:10.3390/ma14154176

Lv, T., Zhang, J., Hou, D., Long, W.-J., and Dong, B. (2024a). Mechanical properties and microstructural characteristics of seawater-mixed sintered sludge cement paste. *Constr. Build. Mater.* 414, 134996. doi:10.1016/j.conbuildmat.2024.134996

Lv, T., Zhang, J., Xu, L., Hou, D., Long, W.-J., and Dong, B. (2024c). Hydration behavior and chloride binding of seawater-mixed sintered sludge cement paste: experimental and thermodynamic study. *Constr. Build. Mater.* 426, 136170. doi:10.1016/j.conbuildmat.2024.136170

Lv, T., Zhang, J., Zhao, M., Yang, J., Hou, D., and Dong, B. (2024b). Utilization of sintered sludge ash with different mechanical–thermal activation parameters as a supplementary cementitious material: mechanical properties and life cycle assessment of cement-based paste. *Materials* 17 (16), 4101. doi:10.3390/ma17164101

Mathern, A., and Yang, J. (2021). A practical finite element modeling strategy to capture cracking and crushing behavior of reinforced concrete structures. *Materials* 14 (3), 506. doi:10.3390/ma14030506

Nobre, J., Ahmed, H., Bravo, M., Evangelista, L., and de Brito, J. (2020). Magnesia (MgO) production and characterization, and its influence on the performance of cementitious materials: a review. *Materials* 13 (21), 4752. doi:10.3390/ma13214752

Pavlíková, M., Pivák, A., Záleská, M., Jankovský, O., Reiterman, P., and Pavlík, Z. (2020). Magnesium oxychloride cement composites lightened with granulated scrap tires and expanded glass. *Materials* 13 (21), 4828. doi:10.3390/ma13214828

Ryu, J.-C., Lee, C.-J., Shin, D.-H., and Ko, D.-C. (2024). Prediction of the interface behavior of a steel/CFRP hybrid Part Manufactured by stamping. *Materials* 17 (17), 4291. doi:10.3390/ma17174291

Szewczak, I., Rzeszut, K., Rozylo, P., and Snela, M. (2020). Laboratory and numerical analysis of steel cold-formed sigma beams retrofitted by bonded CFRP Tapes—extended research. *Materials* 13 (21), 4960. doi:10.3390/ma13214960

Tang, H., Qian, J., Ji, Z., Dai, X., and Li, Z. (2020). The protective effect of magnesium phosphate cement on steel corrosion. *Constr. Build. Mater.* 255, 119422. doi:10.1016/j.conbuildmat.2020.119422

Wang, H., Yan, P., and Guan, Y. (2021). Robust heterojunctions of metallic alloy and carbon fiber-reinforced composite induced by laser processing. *Materials* 14 (23), 7469. doi:10.3390/ma14237469

Xiang, D., and Yang, Y. (2023). Study on calculation of bond-slip performance and strength of C50 concrete epoxy coating steel bars. *Industrial Saf. Environ. Prot.* 39 (09), 39–43.

Xiangrui, M., Yu, J., Bing, C., and Liyan, W. (2023). Research progress on the setting time and solidification mechanism of magnesium phosphate cement: a review. *Constr. Build. Mater.* 408, 133612. doi:10.1016/j.conbuildmat.2023.133612

Xiaoming, H., Guodong, L., Yangzezhi, Z., and Haoyuan, L. (2023). The performance of magnesium phosphate cement in negative temperature environment: a state-of-the-art review. *J. Build. Eng.* 76, 107278. doi:10.1016/j.jobe.2023.107278

Xin, W., Xiang, H., Jianming, Y., Linlin, C., and Caijun, S. (2022). Research progress on interfacial bonding between magnesium phosphate cement and steel: a review. *Constr. Build. Mater.* 342 (PB), 127925. doi:10.1016/j.conbuildmat.2022.127925

Yang, H. (2018). Preparation and Modification of magnesium phosphate cement anticorrosive coating on Q235 Steel Surface. *Southwest Jiaot. Univ.*

Yang, N., Shi, C., Yang, J., and Chang, Y. (2013). Research progresses in magnesium phosphate cement–based materials. *J. Mater. Civ. Eng.* 26 (10), 04014071. doi:10.1061/(asce)mt.1943-5533.0000971

Yang, Q., Zhang, S., and Wu, X. (2002). Deicer-scaling resistance of phosphate cement-based binder for rapid repair of concrete. *Cem. Concr. Res.* 32 (1), 165–168. doi:10.1016/s0008-8846(01)00651-2

Yang, Q., Zhang, S., Yang, Q., and Wu, X. (2000). Performance of new fast hardening phosphate repair material. *Concr. Cem. Prod.* 04, 8–11.

Yongkang, Z., and Xiaoming, G. (2012). Study on bond performance test of fiber reinforced plastics(FRP) bar and concrete. *Urban Roads Bridg. and Flood Control.*

Zhang, W., Dai, M., Liang, X., Wang, X., Wei, W., and Zhou, Z. (2023). Interfacial enhancement by CNTs grafting towards high-performance mechanical properties of carbon fiber-reinforced epoxy composites. *Materials* 16 (10), 3825. doi:10.3390/ma16103825

Zhao, Y., and Jin, W. (2002). Test study on bond stress-slip relationship of concrete and steel bar. *J. Build. Struct.* 01, 32–37.